DOI: 10.1002/ejic.200900640

Extending the Lindqvist Family to Late 3d Transition Metals: A Rational Entry to CoW_5 Hexametalate Chemistry

R. John Errington,*[a] Gavin Harle,[a] William Clegg,[a] and Ross W. Harrington[a]

Keywords: Polyoxometalates / Lindqvist structures / Tungsten / Cobalt / Mass spectrometry

The dimeric CoW_5 Lindqvist-type anion $[\{CoW_5O_{18}H\}_2]^{6-}$ (**1**) has been obtained as a tetrabutylammonium (TBA) salt by addition of either $[Co(MeCN)_4(H_2O)_2]^{2+}$ or $CoCl_2$ to a "virtual" $W_5O_{18}^{6-}$ precursor generated by non-aqueous hydrolysis of a mixture of $(TBA)_2WO_4$ and $WO(OMe)_4$. Analysis of the X-ray crystal structure of $(TBA)_7$**1**(BF_4) by using the Bond Valence Sum (BVS) method reveals that cobalt is present as Co^{II} and that two protons are associated with CoOW bridging oxygen atoms, one of which is located in a hydrogen bond between the two CoW_5O_{18} units, whereas the other is disordered between an adjacent oxygen atom and its symmetry-related site on the other CoW_5O_{18} unit. Treatment with pyridine cleaves dimer **1** to give $[(py)CoW_5O_{18}H]^{3-}$ (**2**), and the single protonated CoOW site was identified by BVS analysis of an X-ray crystal structure. Due to the higher anionic charge of $[CoW_5O_{18}]^{4-}$, bands due to terminal $\nu_{W=O}$ in the FTIR spectra of **1** and **2** are shifted to lower wavenumbers (933 and 935 cm^{-1}, respectively) compared to those of $[W_6O_{19}]^{2-}$ (974 cm^{-1}) and group 4 derivatives $[(X)MW_5O_{18}]^{3-}$ (945–955 cm^{-1}), despite protonation of the oxometalate framework. Peaks due to CoW_5 oxometalates dominate the electrospray ionisation mass spectra of $(TBA)_7$**1**(BF_4) and $(TBA)_3$**2**, the most intense being assigned to $\{CoW_5O_{17}\}^{2-}$, which is formally derived from $[CoW_5O_{18}H]^{3-}$ by protonation and loss of H_2O.

Introduction

The design and assembly of polyoxometalates (POMs) with pre-determined composition, size, shape and functionality remains the ultimate goal in this rich and diverse area of chemistry.[1] In order to achieve this ideal scenario, the complex dynamic processes involved in aggregation and the factors affecting the relative stabilities of the various structural motifs must be well understood in order to provide the basis for reliable and predictable synthetic methodologies. To date, the most frequently adopted approach to rational heterometallic POM synthesis has been to incorporate the heterometal(s) into pre-formed lacunary structures, which are almost invariably derivatives of either Keggin-type $[EM_{12}O_{40}]^{n-}$ or Wells–Dawson-type $[E_2M_{18}O_{62}]^{n-}$ structures.[1,2] In contrast, the ab initio assembly of POM structures remains a major challenge, although certain complex systems can be manipulated with some degree of predictability. For example, Müller has proposed that acidified aqueous molybdate solutions are pre-disposed towards the formation of pentagonal $MoMo_5$ building blocks which, in the presence of appropriate linking units, assemble into large spherical "Keplerate" polymolybdates, and has now demonstrated that tungstate systems can be deliberately induced to form similar structures containing WW_5 building blocks.[3] Cronin has highlighted advances in the design and assembly of POMs and the potential for creating functional systems.[4]

Following the pioneering work of Jahr and Fuchs, who demonstrated that POMs can be obtained by the alkaline hydrolysis of metal alkoxides,[5] our efforts to develop rational methods for synthesis that facilitate systematic manipulation of POM functionality and detailed studies of solution reactivity have exploited the inherent stability of the Lindqvist hexametalate structure in non-aqueous media, and we have obtained a range of alkoxido hexametalates $[(RO)MW_5O_{18}]^{n-}$ (M = Ti, Zr, Hf) by hydrolytic aggregation.[6] The alkoxido group in these anions can be systematically replaced by a wide variety of other ligands in straightforward exchange reactions with protic reagents.[7] This reactivity also enabled us to attach TiW_5 hexametalates to derivatised silicon surfaces in the first demonstration of covalent surface immobilisation of POMs.[8] Scheme 1 illustrates this methodology and indicates how it has been extended to group 5 analogues by adjusting the reaction stoichiometry.

The analogy between POMs and solid-state oxides and the importance of later transition metals in heterogeneous catalysis led us to investigate whether our non-aqueous methods would enable us to incorporate these metals into POM structures in a directed manner. Molecular oxides of

[a] School of Chemistry, Bedson Building, Newcastle University, Newcastle upon Tyne, NE1 7RU, UK
Fax: +44-191-222-6929
E-mail: John.Errington@ncl.ac.uk

Supporting information for this article is available on the WWW under http://dx.doi.org/10.1002/ejic.200900640.

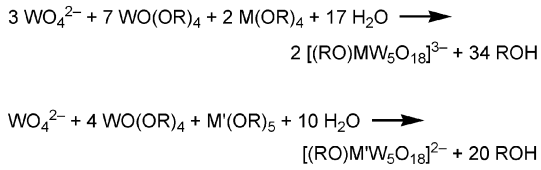

Scheme 1. Synthesis of heterometallic alkoxido Lindqvist anions (M = Ti, Zr, Hf; M′ = Nb, Ta).

this type provide soluble models for heterogeneous oxide catalysts and by studying their reactivity in solution we hope to gain a greater mechanistic understanding of important catalytic processes and develop more efficient and selective catalysts. Metals from groups 8 to 11 have been incorporated into Keggin-type POMs and larger structures constructed from various fragments of Keggin units,[9] but substitution into Lindqvist structures has been limited to the electrophilic metals from groups 4, 5, 6 and 14.[6,7,10] "Sandwich" structures $[Pd_2(W_5O_{18})_2]^{8-}$ and $[Ag_2\{Mo_5O_{13}(OMe)_4(NO)\}_2]^{4-}$ containing square-planar Pd^{II} or Ag^{I} have been reported,[11] although in these cases the metals are bonded *exo* to the W_5 cage rather than in octahedral sites within the structure. In this regard, these group 10 derivatives are similar to the lanthanide complexes $[Ln(W_5O_{18})_2]^{9-}$, which were first characterised by Weakley and co-workers.[12] For the attempted synthesis of cobalt-substituted Lindqvist-type tungstates $[LCoW_5O_{18}]^{4-}$ we adopted a stepwise strategy involving the initial generation of the lacunary anion $W_5O_{18}^{6-}$ and its subsequent reaction with a Co^{II} salt. Although this pentatungstate ligand has never been isolated and characterised as an independent species, its kinetic stability in solution was established by Pope, who demonstrated the transfer of the $W_5O_{18}^{6-}$ "ligand" from La^{III} to Ce^{III} in aqueous solution.[13] We have now established that Lindqvist-type hexametalates containing later transition metals are accessible from a "virtual" $W_5O_{18}^{6-}$ precursor prepared by a non-aqueous hydrolytic reaction, and describe here the synthesis and structural characterisation of two CoW_5 heterometalates and evidence for the formation of an analogous FeW_5 species.

Results and Discussion

Synthesis

The CoW_5 Lindqvist dimer $[\{CoW_5O_{18}H\}_2]^{6-}$ (**1**) was obtained from a tungstate precursor which was formed in an attempt to prepare the lacunary pentatungstate $W_5O_{18}^{6-}$ by stoichiometric hydrolysis of a 3:2 mixture of $(TBA)_2WO_4$ and $WO(OMe)_4$ in MeCN as in Scheme 2. A more detailed investigation of the product from this reaction will be described elsewhere, but it is clearly not a single compound and its colour varied from pale to darker yellow in different batches. The only previously reported yellow isopolytungstate is $[W_{10}O_{32}]^{4-}$. The ^{183}W and ^{17}O NMR spectra of this hydrolysis product are indicative of a mixture and contained many more peaks than expected for the lacunary $W_5O_{18}^{6-}$, none of which correspond to reported chemical shifts for $[W_{10}O_{32}]^{4-}$. The reaction between this "virtual" $W_5O_{18}^{6-}$ precursor and $[Co(MeCN)_4(H_2O)_2](BF_4)_2$ in MeCN gave a purple-blue crystalline product in only moderate yield due to its high solubility in MeCN and the difficulty in separating it from the $(TBA)BF_4$ by-product, which co-crystallised with $(TBA)_6$**1**. This dimeric CoW_5 POM dissolved in pyridine to give a dark pink solution of the monomeric pyridine adduct $[(py)CoW_5O_{18}H]^{3-}$ (**2**), which was precipitated as its TBA salt by addition of diethyl ether and recrystallised by slow concentration of a dichloromethane solution under a stream of nitrogen. It was difficult to remove all traces of the mother liquor from the well-formed crystals of $(TBA)_3$**2** because of their high solubility, and representative microanalytical data were therefore problematic.

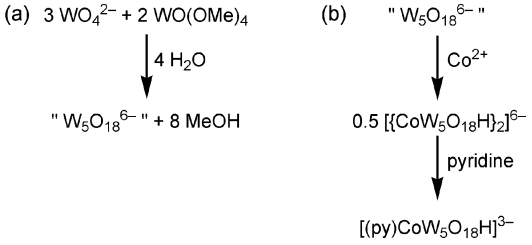

Scheme 2. Synthesis of "virtual" $W_5O_{18}^{6-}$ (a) and of CoW_5 polyoxometalates with the Lindqvist structure (b).

X-ray Crystal Structures

The structure of **1** from a single-crystal X-ray diffraction study of the double salt $(TBA)_7$**1**(BF_4) is shown in Figure 1. Bond-valence parameters developed for solids are useful for calculating metal oxidation states and locating protonation sites in POMs,[7a,14] because hydrogen atoms cannot be reliably located in complexes of heavy metals by X-ray diffraction. By applying the procedure and parameters provided by Altermatt and Brown and later by Brese and O'Keeffe to determine the oxidation state of cobalt, we obtained $V_{Co} = 2.0$.[15] From the number of TBA cations, this would require two protons to be associated with this dimeric anion, and from oxygen bond valence sum calculations these appear to be localised at O16 and O17 ($V_{O16} = 1.38$ and $V_{O17} = 1.37$, respectively). The O16···O16A distance of 2.731 Å indicates that one proton is located in a hydrogen bond between these atoms, whereas the other proton is disordered over O17 and O17A due to the C_2 symmetry of the anion in the crystal structure (atoms with suffix A are related to atoms in the asymmetric unit by this crystallographic symmetry). The longest Co–O bond length is 2.262(6) Å to the central oxygen atom O18, and the shortest is the bridging bond to O15A at 2.002(7) Å, whereas the Co–O15 bond length of 2.193(8) Å is longer than the distances to O14, O16 and O17, which range from 2.052 to 2.074 Å. This is a little surprising in that, given the general stability of Lindvist hexametalate structures, the shortest bonds might have been expected to be within the $\{CoW_5O_{18}\}$ core rather than between the two units. As observed in other MW_5

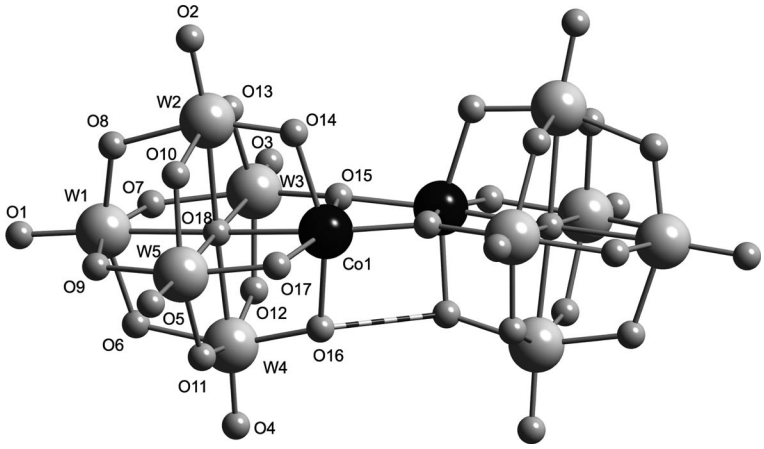

Figure 1. View of the anion **1** showing the proposed hydrogen-bonding interaction between O16 and O16A.

Lindqvist structures, the presence of the heterometal distorts the tungstate framework from the symmetrical $[W_6O_{19}]^{2-}$ structure. For the four equatorial tungsten atoms W2 to W5 the W–O(Co) bonds are shorter than the *trans*-W–O(W1) bonds, although the presence of protons at O16 and O17 reduces the difference for W4 and W5. The average terminal W=O bond length of 1.709 Å is similar to those in other $[(X)MW_5O_{18}]^{3-}$ hexametalates and longer than those in $[W_6O_{19}]^{2-}$ (1.69 Å), reflecting the higher charge on these heterometalates.

The crystal structure of the apparently hydrated dichloromethane solvate of the pyridine adduct $(TBA)_3$**2**·$0.5CH_2Cl_2$·$0.33H_2O$ contained three independent anions in the asymmetric unit, one of which is shown in Figure 2, together with nine cations, one and a half molecules of dichloromethane, and one water molecule (assigned as such on the basis of electron density and intermolecular distances). The $\{CoW_5O_{18}\}$ framework of **2** shows similar features to that of **1**. Using bond valence parameters for O and N, the calculated V_{Co} values ranged from 2.18 to 2.26 for the three independent polyanions in the structure, confirming an oxidation state of Co^{II}. The cobalt environment is more symmetric in **2** than in **1** with four similar Co–O(W) bridging distances to equatorial tungsten atoms and Co–N bond lengths of 2.052(13), 2.028(12) and 2.025(15) Å. Oxygen bond valence sums indicate that the proton in **2** is localised on O7 (V_{O7} = 1.10), and this proton is clearly not sufficiently acidic to be removed by pyridine. The W–O(Co) bonds for the equatorial tungsten atoms W1, W3 and W4 are longer than the *trans*-W–O(W5) bonds, but this situation is reversed for W2, with W2–O(W5) >W(2)–O(Co) due to protonation of O7; this pattern is observed for all three crystallographically independent anions, the protonated oxygen atoms in the other two anions being O28 and O45. Consistent with the 3-charge, terminal W=O bond lengths are similar to those in **1**.

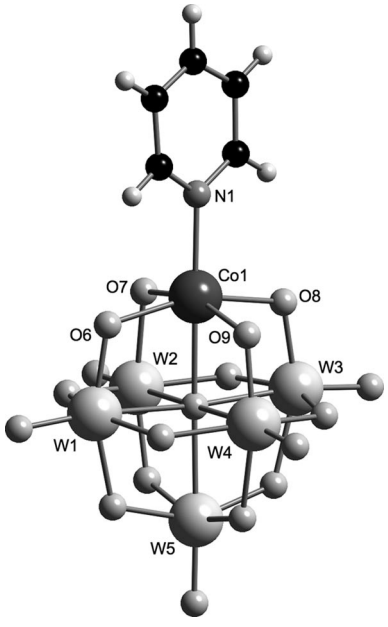

Figure 2. View of one of the three independent anions in the crystal structure of solvated $(TBA)_3$**2**.

Electrospray Ionisation Mass Spectrometry

The negative-ion electrospray ionisation (ESI) mass spectra of $(TBA)_7$**1**(BF_4) and $(TBA)_3$**2** contain a range of peaks for CoW_5 ions (Tables 1 and 2), and the most intense ion cluster pattern is for $\{CoW_5O_{17}\}^{2-}$ (Figure 3). Notably, no ions containing pyridine are present in the mass spectrum of $(TBA)_3$**2**. A cluster of peaks for $W_6O_{19}^{2-}$ appears at *m*/*z* = 703.79 in the spectrum of $(TBA)_7$**1**(BF_4) but not in that of $(TBA)_3$**2**, and we have yet to determine whether this is due to a small amount of impurity or to the instability of **1** under electrospray conditions. Peaks for the parent monomer $[CoW_5O_{18}H]^{3-}$ are not present in either mass spectrum, but it is easy to envisage protonation and elimination of H_2O from the resulting $[CoW_5O_{18}H_2]^{2-}$ to give $\{CoW_5O_{17}\}^{2-}$. A more detailed analysis of ESMS data will be published elsewhere, but the prevalence of peaks due to CoW_5 species suggests that this structural unit has significant stability in solution and under ESIMS conditions, and

investigations are underway to explore the implications of these observations regarding the reactivity of the $\{CoW_5O_{18}H\}^{3-}$ oxometalate core.

Table 1. $\{CoW_5\}$ ion assignments in the negative-ion electrospray ionisation mass spectrum of $(TBA)_7\mathbf{1}\cdot BF_4$.

Ion	*m*/*z* (observed)	*m*/*z* (calculated)
$\{CoW_5O_{17}\}^{2-}$	625.29	625.30
$\{CoW_5O_{19}\}^{2-}$	641.31	641.30
$\{CoW_5O_{21}H_8\}^{2-}$	661.31	661.32
$\{CoW_5O_{19}H\}^{-}$	1283.64	1283.60
$\{(TBA)(CoW_5O_{19})\}^{-}$	1524.96	1524.88

Table 2. $\{CoW_5\}$ ion assignments in the negative-ion electrospray ionisation mass spectrum of $(TBA)_3\mathbf{2}$.

Ion	*m*/*z* (observed)	*m*/*z* (calculated)
$\{W_4O_{13}\}^{2-}$	471.89	471.87
$\{CoW_4O_{14}\}^{2-}$	509.36	509.33
$\{CoW_5O_{17}\}^{2-}$	625.32	625.30
$\{CoW_5O_{19}\}^{2-}$	641.30	641.30
$\{CoW_5O_{21}H_8\}^{2-}$	661.31	661.32
$\{Co_2W_{10}O_{35}H_3\}^{3-}$	840.10	840.07
$\{(TBA)(Co_2W_{10}O_{35}H_2)\}^{3-}$	920.54	920.50
$\{(TBA)(W_4O_{13})\}^{-}$	1186.04	1186.02
$\{(TBA)(CoW_4O_{14})\}^{-}$	1260.90	1260.95
$\{CoW_5O_{19}H\}^{-}$	1283.61	1283.60
$\{(TBA)(CoW_5O_{19})\}^{-}$	1524.72	1524.88

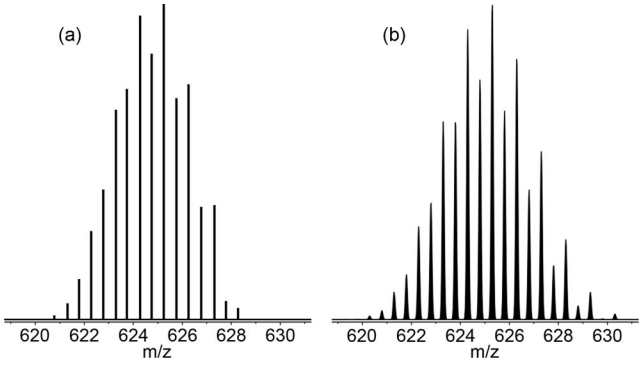

Figure 3. Peak pattern for the ion cluster assigned to $\{CoW_5O_{17}\}^{2-}$ in the negative-ion electrospray mass spectrum of $(TBA)_7\mathbf{1}(BF_4)$ (a) and the simulated pattern for this ion (b).

FTIR Spectra

FTIR spectra of $(TBA)_7\mathbf{1}(BF_4)$ and $(TBA)_3\mathbf{2}$ are shown in Figure 4. The key feature of these spectra is that the bands associated with $\nu_{W=O}$ at 933 and 935 cm^{-1} for **1** and **2**, respectively, are at significantly lower wavenumbers than the analogous band for $[W_6O_{19}]^{2-}$ (974 cm^{-1}) because of the higher anionic charge of the CoW_5 hexametalates. These values are even lower than those for group 4 derivatives $[(X)MW_5O_{18}]^{3-}$, which lie in the range 945–955 cm^{-1}.[6,7] This may be due to the less electrophilic nature of cobalt compared to titanium and zirconium, or it might suggest that protonation of the $[LCoW_5O_{18}]^{4-}$ oxometalate unit does not affect the terminal $\nu_{W=O}$ stretching frequencies, which would be expected to be lower than those for the group 4 derivatives. The larger number of strong bands associated with bridging vibrations in the spectra of **1** and **2** between 820 and 660 cm^{-1} compared with the spectra of titanium and zirconium derivatives may be due to the lower symmetry arising from protonation and/or dimerisation of the $[CoW_5O_{18}]^{4-}$ oxometalate. In the spectrum of **1**, a band at 606 cm^{-1}, which is not present in the spectrum of **2**, may be associated with vibration of the Co_2O_2 ring formed as a result of dimerisation. In addition, the ν_{BF} band for BF_4^- in $(TBA)_7\mathbf{1}(BF_4)$ is evident at 1055 cm^{-1}, whereas a weak band at ca. 1600 cm^{-1} in the spectrum of **2** is assigned to pyridine. The FTIR spectrum of the product from the reaction with $CoCl_2$ was the same as that for $(TBA)_7\mathbf{1}(BF_4)$ except for the absence of a ν_{BF} absorption, which is consistent with the formulation $(TBA)_7\mathbf{1}(Cl)$ derived from an X-ray crystal structure determination, which, although of low quality, was sufficient to identify the oxometalate core and the presence of the extra TBA cation and chlorido ions.

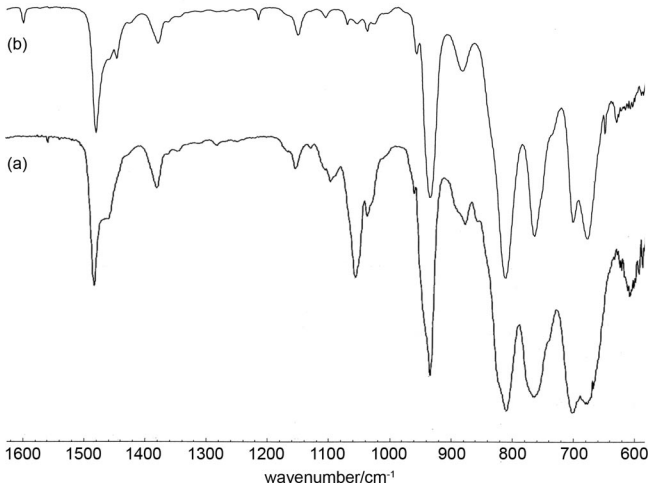

Figure 4. Transmittance FTIR spectra of $(TBA)_7\mathbf{1}(BF_4)$ (a) and $(TBA)_3\mathbf{2}$ (b) in the region 600–1600 cm^{-1}.

NMR Spectra

An advantage of our non-aqueous hydrolytic approach to POM synthesis is that ^{17}O enrichment of the metal oxide framework is readily achieved by using the same synthetic procedure, but with stoichiometric amounts of ^{17}O-enriched water for the hydrolysis. The ^{17}O NMR spectra of ^{17}O-enriched samples of **1** and **2** are shown in Figure 5 and are markedly different. Not only are there more peaks in the spectrum of **1**, but the peaks in the spectrum of **2** are significantly broader. Note that peak intensities are affected by the hydrolytic aggregation mechanism, details of which are currently unknown, but some sites are likely to be more readily enriched than others. In solution, the two halves of **1** will be non-equivalent if the solid-state structure is retained because of the nature of the hydrogen bonding. One half will provide the hydrogen atom on O16 for the hydrogen bond to O16A, which means that the other half will be

protonated at O17A (in the crystal structure, the crystallographic symmetry introduces disorder and makes the two halves equivalent on average). Ten high-frequency peaks would therefore be expected for terminal W=O, and this appears to be the case between δ = 733 and 880 ppm. The peaks at δ = 576, 573 and 537 ppm in the spectrum of **1** appear to be due to μ_3-O linking the two halves of the dimer as indicated in Figure 5 (a), as there are no equivalent peaks in the ^{17}O NMR spectrum of monomeric **2**. This would mean that the peaks for μ_2-CoOW are either those at $\delta \approx$ 700 ppm or those at $\delta \approx$ 450 ppm. Lower-frequency peaks are likely to be associated with WOW bridging oxygen atoms, and there are no obvious peaks for the central μ_6-O. The possibility that the complexity of the ^{17}O NMR spectrum of **1** is due to dissociation in solution cannot be ruled out, but the fact that the CoW_5 structure is retained upon dissolution in pyridine and does not dissociate to give the $[Co(py)_6]^{2+}$ cation and miscellaneous tungstate species would suggest that the CoW_5 core is retained upon dissolution in MeCN. We have not measured the magnetic properties of **1** and **2**, but the broad peaks in the ^{17}O NMR spectrum of **2** would indicate a larger paramagnetic effect in the monomeric ion, so there is likely to be some magnetic interaction between the two cobalt atoms in **1**. In the ^{1}H NMR spectrum of $(TBA)_7$**1**(BF_4) the TBA peaks are broadened with chemical shifts of δ = 0.66, 0.78, 1.27 and 1.95 ppm, which are lower than usual due to the paramagnetism of the sample. Small singlets at δ = 4.18 and 5.48 and 12.63 ppm may be due to OH, the much broader downfield peak being tentatively assigned to the hydrogen-bonded site. In addition to upfield-shifted TBA peaks, the ^{1}H NMR spectrum of $(TBA)_3$**2** contains broad peaks between δ = 7 and 9 ppm, presumably due to pyridine, and a broadened peak at δ = 10.90 ppm, which is tentatively assigned to OH.

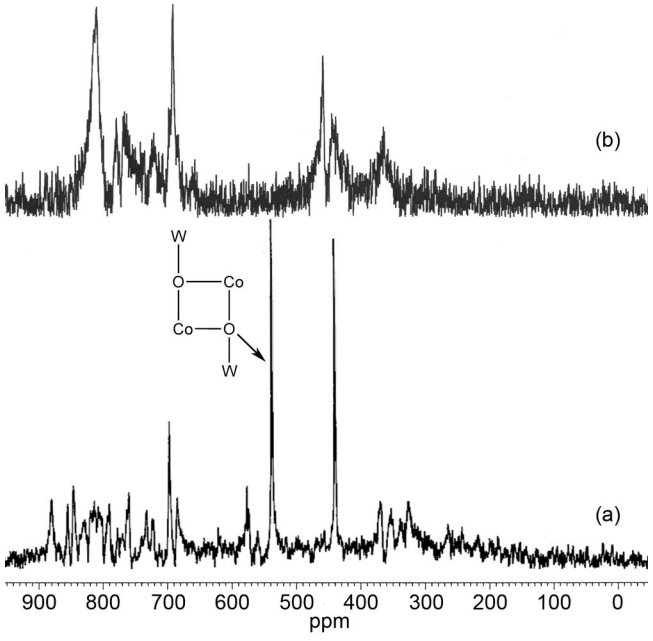

Figure 5. ^{17}O NMR spectra of $(TBA)_7$**1**BF_4 (a) and $(TBA)_3$**2** (b) in MeCN, indicating the proposed peak assignment for oxygen atoms linking the two hexametalate units in dimer **1**.

Summary and Conclusions

We have established that the deliberate synthesis of CoW_5 Lindqvist-type POMs containing late 3d transition metals is possible by a two-step methodology that involves preliminary preparation of a tungstate precursor with a charge/metal ratio equivalent to the putative lacunary species $W_5O_{18}^{6-}$. Although initial analysis suggests that this precursor is a mixture, it behaves in a constitutionally dynamic fashion in solution,[16] forming Lindqvist-type $[(L)MW_5O_{18}]^{n-}$ heterometalates when treated with MCl_x or labile complexes of M^{x+}. With $[Co(MeCN)_4(H_2O)_2]^{2+}$ or $CoCl_2$ the dimeric $[\{CoW_5O_{18}H\}_2]^{6-}$ (**1**) is formed, and the crystal structure of $(TBA)_7$**1**(BF_4) has been determined. X-ray diffraction data for $(TBA)_6$**1**(Cl) were of lower quality, but the structure nevertheless showed the presence of **1** and chlorido ions, and the FTIR spectrum was the same as that of $(TBA)_7$**1**(BF_4), except for the absence of a peak for ν_{BF}. The hexanuclear structure is retained upon cleavage of the dimer with pyridine to give the adduct $[(py)CoW_5O_{18}H]^{3-}$ (**2**), and the oxidation state of cobalt and the location of the surface protons in **1** and **2** were determined by the Bond Valence Sum method. We are now exploring the scope of this synthetic method and investigating the properties of the new MW_5 POMs in detail. Preliminary results indicate that FeW_5 analogues are accessible by treating the $\{W_5O_{18}\}^{6-}$ virtual precursor with $FeCl_3$, and these will be described elsewhere.

Experimental Section

General Considerations: Reactions and manipulations involving air/moisture-sensitive compounds were routinely carried out under dry, oxygen-free nitrogen by using standard Schlenk and dry-box techniques.[17] Reactions at elevated temperatures were carried out in sealed, screw-top Schlenk flasks fitted with PTFE screw valves (Young's valves). All other reactions and manipulations were carried out by using standard bench-top techniques. Solvents were dried with and distilled from appropriate desiccants. Diethyl ether was dried with and distilled from sodium/benzophenone, acetonitrile and dichloroemthane were dried with and distilled from calcium hydride, and ethyl acetate was dried by storage over molecular sieves (3 Å). $(TBA)_2WO_4$[10g] and $WO(OMe)_4$[18] were prepared as described previously, and $[Co(MeCN)_4(H_2O)_2](BF_4)_2$ was prepared from $Co(acac)_2$ by treatment with $HBF_4{\cdot}OEt_2$ in MeCN.[19] Samples enriched in ^{17}O were prepared by using 10% ^{17}O-enriched water (Goss Scientific Instruments) for hydrolysis. ^{17}O NMR spectra were acquired with a Jeol Lamda 500 spectrometer operating at 67.8 MHz. ESI mass spectra were recorded with a Waters LCT Premier LC-MS spectrometer by direct insertion of samples using the following conditions: capillary voltage 5000 V; sample cone voltage 35 V; desolvation temperature 20 °C; source temperature 90 °C. FTIR spectra were recorded from powders with a Varian 800 FT-IR spectrometer fitted with an ATR attachment. Elemental

analyses were performed by Newcastle University Chemical Analysis Service.

X-ray Crystallography: Data were collected at 150 K with an Oxford Diffraction Gemini A Ultra diffractometer by using Mo-K_α radiation (λ = 0.71073 Å). Semiempirical absorption corrections, together with frame-scaling for intensity variations, were made on the basis of repeated and symmetry-equivalent reflections.[20] The structures were solved by standard direct methods and refined by full-matrix least squares on all unique F^2 values.[21] Restraints were applied to molecular geometry and anisotropic displacement parameters of the lighter atoms. Hydrogen atoms, except for those on the anion cages and on a water molecule, which were not located, were placed in idealised positions and refined as riding. Both structures may contain unresolved disorder, but this does not affect the anions. Summary of principal crystallographic data for $(TBA)_7$**1**(BF_4): M = 4318.4, orthorhombic, $P2_12_12$, a = 24.3778(3), b = 17.0185(2), c = 18.1359(3) Å, V = 7524.11(18) Å^3, Z = 2; R_{int} = 0.039, R (F, 10206 observed data) = 0.041, R_w (F^2, all data) = 0.088 for 13620 unique data, 771 refined parameters and 649 restraints. For $(TBA)_3$**2**·0.5CH_2Cl_2·0.33H_2O: M = 2122.1, monoclinic, $P2_1$, a = 15.3509(2), b = 23.6647(4), c = 30.2424(5) Å, V = 10631.3(3) Å^3, Z = 6; R_{int} = 0.076, R (F, 22036 observed data) = 0.046, R_w (F^2, all data) = 0.069 for 36313 unique data, 2246 refined parameters and 6966 restraints. An absolute structure parameter was satisfactorily refined for each structure, as they are both non-centrosymmetric.[22] CCDC-738733 [$(TBA)_7$**1**(BF_4)] and -738734 [$(TBA)_3$**2**·0.5CH_2Cl_2·0.33H_2O] contain the supplementary crystallographic data for this paper. These data can be obtained free of charge from The Cambridge Crystallographic Data Centre via www.ccdc.cam.ac.uk/data_request/cif.

Preparation of the "Virtual" Precursor "$(TBA)_6W_5O_{18}$": A solution of $WO(OMe)_4$ (0.56 g, 1.73 mmol) in acetonitrile (15 mL) was added to a solution of $(TBA)_2WO_4$ (1.90 g, 2.59 mmol) in acetonitrile (15 mL) with stirring. The resulting solution was heated at 90 °C for 90 min, then allowed to cool to ambient temperature before addition of water (62.5 μL, 3.47 mmol) with stirring. After heating at 90 °C for 12 h, the volatiles were removed under reduced pressure to leave a yellow oily residue, which was triturated with diethyl ether (5 × 20 mL) to give an orange-yellow solid which was dried in vacuo. Yield 2.25 g, 98% based on $(TBA)_6W_5O_{18}$. FTIR: $\tilde{\nu}$ = 2960 (m), 2924 (m), 2873 (m), 1642 (w), 1485 (m), 1395 (w), 1153 (w), 1104 (w), 1058 (w), 1031 (w), 919 (m), 868 (m), 811 (s), 788 (s), 729 (m), 697 (s) cm^{-1}. ^{17}O NMR (67.8 MHz, CH_3CN, 23 °C): δ = 671, 663, 643, 636, 603, 442, 331, 298 ppm. ^{183}W NMR (20.84 MHz, CH_3CN, 23 °C): δ = 62.3, 53.0, 48.1, 38.6, 12.7, 10.3, –4.1, –8.6, –10.2, –27.3, –31.8, –39.0, –41.9, –43.4, –74.7, –95.1 ppm.

Preparation of $(TBA)_7[\{CoW_5O_{18}H\}_2](BF_4)$ [$(TBA)_7$1**(BF_4)]:** Half of the precursor prepared as above (1.12 g, ca. 2.1 mmol of W) was dissolved in MeCN (20 mL) to give a golden-yellow solution, to which was added a solution of $[Co(MeCN)_4(H_2O)_2](BF_4)_2$ (0.18 g, 0.42 mmol) in MeCN (10 mL). The resulting deep blue-purple solution was stirred for 12 h, and the volume of the solution was then reduced to approximately 10 mL under reduced pressure. The product obtained after addition of diethyl ether and storage in a freezer at –20 °C was further recrystallised from dichloromethane/ethyl acetate to give a blue-purple crystalline solid (0.28 g, 15%). $C_{112}H_{254}BCo_2F_4N_7O_{36}W_{10}$ (4318.35): calcd. C 31.15, H 5.93, N 2.27; found C 31.57, H 5.87, N 2.44. FTIR: $\tilde{\nu}$ = 2960 (m), 2924 (m), 2872 (m), 1483 (m), 1380 (w), 1055 (m), 933 (s), 886 (w), 809 (s), 763 (s), 700 (s), 676 (s), 606 (m) cm^{-1}. ^{17}O NMR (67.8 MHz, CH_3CN, 23 °C): δ = 880. 855, 846, 820, 802, 793, 790. 763, 733, 697, 685, 576, 537, 439, 369, 367, 352, 338, 325 ppm.

Preparation of $(TBA)_7[\{CoW_5O_{18}H\}_2](Cl)$ [$(TBA)_7$1**(Cl)]:** Half of the precursor prepared as above (1.12 g, ca. 2.1 mmol of W) was dissolved in MeCN (20 mL) to give a golden-yellow solution, to which was added a solution of $CoCl_2$ (0.055 g, 0.42 mmol) in acetonitrile (10 mL). After stirring for 12 h, the volume of the resulting dark blue solution was reduced to approximately 10 mL, and a diethyl ether layer was added. Blue-purple crystals were formed on the side of the flask over time (0.20 g, 11%). IR: $\tilde{\nu}$ = 2960 (m), 2924 (m), 2872 (m), 1483 (m), 1381 (w), 1055 (w), 932 (s), 891 (w), 809 (s), 763 (s), 701 (s), 676 (s) cm^{-1}.

Preparation of $(TBA)_3[(C_5H_5N)CoW_5O_{18}H]\cdot CH_2Cl_2\cdot H_2O$ [$(TBA)_3$2**·$CH_2Cl_2\cdot H_2O$]:** $(TBA)_7$**1**(BF_4) (0.10 g, 0.023 mmol) was dissolved in pyridine (5 mL) to give a dark pink solution. Addition of diethyl ether (15 mL) gave a pink precipitate, which was isolated by filtration and dried in vacuo. The solid was dissolved in dichloromethane (2 mL), and crystals were obtained by slow evaporation of the solvent under a stream of nitrogen. $C_{54}H_{118}Cl_2CoN_4O_{19}W_5$ (2176.58): calcd. C 29.80, H 5.46, N 2.57; found C 29.67, H 5.82, N 2.63. ^{17}O NMR (67.8 MHz, CH_3CN, 23 °C): δ = 815, 760, 717, 692, 459, 362 ppm. FTIR: $\tilde{\nu}$ = 2959 (m), 2924 (m), 2872 (m), 1482 (m), 1380 (w), 1055 (w), 958 (w), 935 (s), 883 (w), 812 (s), 765 (s), 701 (s), 678 (s) cm^{-1}.

Supporting Information (see footnote on the first page of this article): ESIMS spectra for $(TBA)_7$**1**(BF_4) and $(TBA)_3$**2**.

Acknowledgments

We thank the UK Engineering and Physical Sciences Research Council for equipment funding (grant EP/F036376X/1) and for a CASE studentship to G. H. We also thank Davy Process Technology for funding as part of the CASE studentship.

[1] a) M. T. Pope, *Heteropoly and Isopoly Oxometalates*, Springer-Verlag, Berlin, **1983**; b) M. T. Pope, A. Müller, *Angew. Chem. Int. Ed. Engl.* **1991**, *30*, 34–48; c) *Polyoxometalates: From Platonic Solids to Anti-Retroviral Activity* (Eds.: M. T. Pope, A. Müller), Kluwer, Dordrecht, The Netherlands, **1994**; d) C. L. Hill, *Chem. Rev.* **1998**, *98*, 1–389 (an issue dedicated to polyoxometalate chemistry); e) *Polyoxometalate Chemistry: From Topology via Self-Assembly to Applications* (Eds.: M. T. Pope, A. Müller), Kluwer, Dordrecht, The Netherlands, **2001**; f) *Polyoxometalate Chemistry for Nano-Composite Design* (Eds.: T. Yamase, M. T. Pope), Kluwer, Dordrecht, The Netherlands, **2002**; g) *Polyoxometalate Molecular Science* (Eds.: J. J. Borrás-Almenar, E. Coronado, A. Müller, M. T. Pope), Kluwer, Dordrecht, The Netherlands, **2004**; h) M. T. Pope in *Comprehensive Coordination Chemistry II* (Eds.: J. A. McCleverty, T. J. Meyer), Elsevier, Amsterdam, **2004**, vol. 4, pp. 635–678.

[2] a) L. C. W. Baker, J. S. Figgis, *J. Am. Chem. Soc.* **1970**, *92*, 3794–3797; b) A. M. V. Cavaleiro, J. D. Pedrosa de Jesus, H. I. S. Noguera in *Metal Clusters in Chemistry* (Eds.: P. Braunstein, P. Raithby, L.Oro), Wiley-VCH, London, **1999**, vol. 1, p. 444.

[3] a) C. Schäffer, A. Merca, H. Bögge, A. M. Todea, M. L. Kistler, T. Liu, R. Thouvenot, P. Gouzerh, A. Müller, *Angew. Chem. Int. Ed.* **2009**, *48*, 149–153; b) A. M. Todea, A. Merca, H. Bögge, T. Glaser, L. Engelhardt, R. Prozorov, M. Lubanc, A. Müller, *Chem. Commun.* **2009**, 3351–3353.

[4] D.-L. Long, E. Burkholder, L. Cronin, *Chem. Soc. Rev.* **2007**, *36*, 105–121.

[5] K. F. Jahr, J. Fuchs, *Chem. Ber.* **1963**, *96*, 2457–2459.

[6] W. Clegg, M. R. J. Elsegood, R. J. Errington, J. Havelock, *J. Chem. Soc., Dalton Trans.* **1996**, 681–690.

[7] a) R. J. Errington, S. S. Petkar, P. S. Middleton, W. McFarlane, W. Clegg, R. A. Coxall, R. W. Harrington, *J. Am. Chem. Soc.* **2007**, *129*, 12181–12196; b) R. J. Errington, S. S. Petkar, P. S.

Middleton, W. McFarlane, W. Clegg, R. W. Harrington, *Dalton Trans.* **2007**, 5211–5222.
[8] R. J. Errington, S. S. Petkar, B. R. Horrocks, A. Houlton, L. H. Lie, S. N. Patole, *Angew. Chem. Int. Ed.* **2005**, *44*, 1254–1257.
[9] Whereas examples containing first-row elements from groups 8–11 in their "usual" oxidation states are well established, attention has recently turned to the heavier congeners and in particular to the stabilisation of higher oxidation states by the oxide framework of POMs. See for example: a) A. E. Kuznetsov, Y. V. Geletii, C. L. Hill, K. Morokuma, D. G. Musaev, *J. Am. Chem. Soc.* **2009**, *131*, 6844–6854; b) U. Lee, H.-C. Joo, K.-M. Park, S. Sankar Mal, U. Kortz, B. Keita, L. Nadjo, *Angew. Chem. Int. Ed.* **2008**, *47*, 793–796; c) M. Sadakane, D. Tsukuma, M. H. Dickman, B. S. Bassil, U. Kortz, M. Capron, W. Ueda, *Dalton Trans.* **2007**, 2833–2838; d) R. Cao, T. M. Anderson, P. M. B. Piccoli, A. J. Schultz, T. F. Koetzle, Y. V. Geletii, E. Slonkina, B. Hedman, K. O. Hodgson, K. I. Hardcastle, X. Fang, M. L. Kirk, S. Knottenbelt, P. Kögerler, D. G. Musaev, K. Morokuma, M. Takahashi, C. L. Hill, *J. Am. Chem. Soc.* **2007**, *129*, 11118–11133; e) T. M. Anderson, R. Cao, E. Slonkina, B. Hedman, K. O. Hodgson, K. I. Hardcastle, W. A. Neiwert, S. Wu, M. L. Kirk, S. Knottenbelt, E. C. Depperman, B. Keita, L. Nadjo, D. G. Musaev, K. Morokuma, C. L. Hill, *J. Am. Chem. Soc.* **2005**, *127*, 11948–11949.
[10] a) C. Flynn Jr, M. T. Pope, *Inorg. Chem.* **1971**, *10*, 2524–2529; b) M. Dabbabi, M. Boyer, *J. Inorg. Nucl. Chem.* **1976**, *38*, 1011–1014; c) M. Filowitz, R. K. C. Ho, W. G. Klemperer, W. Shum, *Inorg. Chem.* **1979**, *18*, 93–103; d) C. Sanchez, J. Livage, J.-P. Launay, M. Fournier, *J. Am. Chem. Soc.* **1983**, *105*, 6817–6823; e) C. J. Besecker, W. G. Klemperer, D. J. Maltbie, D. G. Wright, *Inorg. Chem.* **1985**, *24*, 1027–1032; f) W. G. Klemperer, W. Shum, *J. Chem. Soc., Chem. Commun.* **1979**, 60–61; g) T. M. Che, V. W. Day, L. C. Francesconi, M. F. Fredrich, W. G. Klemperer, W. Shum, *Inorg. Chem.* **1985**, *24*, 4055–4062; h) H. Akashi, J. Chen, T. Sakuraba, A. Yagasaki, *Polyhedron* **1994**, *13*, 1091–1093; i) M. Che, V. W. Day, L. C. Francesconi, M. F. Fredrich, W. G. Klemperer, D. J. Main, A. Yagasaki, O. M. Yaghi, *Inorg. Chem.* **1992**, *31*, 2920–2928.
[11] a) S. J. Angus-Dunne, R. C. Burns, D. C. Craig, G. A. Lawrance, *J. Chem. Soc., Chem. Commun.* **1994**, 523–524; b) R. Villanneau, A. Proust, F. Robert, P. Gouzerh, *Chem. Commun.* **1998**, 1491–1492.
[12] a) R. D. Peacock, T. J. R. Weakley, *J. Chem. Soc. A* **1971**, 1836–1839; b) J. Iball, J. N. Low, T. J. R. Weakley, *J. Chem. Soc., Dalton Trans.* **1974**, 2021–2024.
[13] N. Belai, M. Sadakane, M. T. Pope, *J. Am. Chem. Soc.* **2001**, *123*, 2087–2088.
[14] M. Piepenbrink, M. U. Triller, N. H. J. Gorman, B. Krebs, *Angew. Chem. Int. Ed.* **2002**, *41*, 2523–2525.
[15] a) I. D. Brown, D. Altermatt, *Acta Crystallogr., Sect. B* **1985**, *41*, 244–247; b) N. E. Brese, M. O'Keeffe, *Acta Crystallogr., Sect. B* **1991**, *47*, 192–197.
[16] J.-M. Lehn, *Chem. Soc. Rev.* **2007**, *36*, 151–160.
[17] R. J. Errington, *Advanced Practical Inorganic and Metalorganic Chemistry*, Blackie Academic & Professional, London, **1997**.
[18] W. Clegg, R. J. Errington, P. Kraxner, C. Redshaw, *J. Chem. Soc., Dalton Trans.* **1992**, 1431–1438.
[19] Full details of the preparation and X-ray structural characterisation of this compound will be described elsewhere.
[20] Data collection and processing were carried out with Oxford Diffraction CrysAlisPro software.
[21] Programs for structure solution and refinement were components of Bruker *SHELXTL* software. Structure graphics were produced by using CrystalMaker.
[22] H. D. Flack, *Acta Crystallogr., Sect. A* **1983**, *39*, 876.

Received: July 7, 2009
Published Online: October 30, 2009

